

RESEARCH PAPER

Coupling Plasmon for Gold, Silver and Aluminium Nanostructure Homo- Dimers and Nano-Sphere

Entidhr Malik Hadi ^{1*}, Rosul Mohammed Naji ², Haneen Lateef Khalee ², Noor. Malik Saadoon ³

¹ Physic Medical Determent, College of Science, Al-Nahrain University, Iraq

² Department of Chemical Engineering, University of Technology, Iraq

³ Centre of Nanotechnology and Advanced Material, University of Technology, Iraq

ARTICLE INFO

Article History:

Received 19 January 2025

Accepted 25 March 2025

Published 01 April 2025

Keywords:

FDTD

Homo-Dimer

Localized Surface Plasmon

Resonance

Near-Field Enhancement

ABSTRACT

In the case when predicted LSPR wavelength values of Ag, Al, and Au nano-spheres in homodimer arrangement are equated, FDTD simulations are utilized for studying homo-dimer nano-structures as localized surface plasmon resonance (SPR). Results indicate that silver and aluminum homo-dimer shows higher shift of LSPR when compared to gold homo-dimer. It is interacting with a homo-dimer nanoparticle (NP), which raises the junction's intensity.

How to cite this article

Hadi E., Naji R., Khalee H., Saadoon N. Coupling Plasmon for Gold, Silver and Aluminium Nanostructure Homo- Dimers and Nano-Sphere. J Nanostruct, 2025; 15(2):563-575. DOI: 10.22052/JNS.2025.02.017

INTRODUCTION

An electric field spot from a light source, such as light, excites metal NPs by creating synchronized groups regarding electron oscillations which just happen on their surface. This type of event is referred to as (LSPR). The strength, frequency, and quality of LSPR in metallic particles are directly influenced by the shape, size, refractive index, and metals composition index related to the surrounding atmospheric medium, all of which are related to local environment. The tightly interacting pairs of NPs are the other component that determines the sensitivity of LSPR. [1,2]. The characteristics of metallic NPs—whose composition, shape assembly, and surroundings

greatly affect the response—are among the many parameters which characterize LSPR because of the subject matter. Monolayer that self-assembles or liquid at a distance from a conducting thin film element could change its refractive index, which might be measured with the use of optical method SPR. Because of this, SPR was extensively employed in the research of biomolecule binding interaction, such as ligands and receptors, cDNA probes, antigens, and enzymes. [3]. The SPR effect can be produced by any conductive material, but just thin Ag layers and Au were incorporated into real SPR devices. Au was a popular material in LSPR applications since it is resonant in visible spectra of electro-magnetic spectrum and gives

* Corresponding Author Email: mae.visit.04@uotechnology.edu.iq



off a golden tint. Many metals display surface Plasmon frequencies in ultraviolet range 8eV, very few other transition metals, like aluminium, Co,

or Ni, were frequently observed to exhibit LSPR. Because of the plasma resonance which takes place in the visible region of the spectra and gives

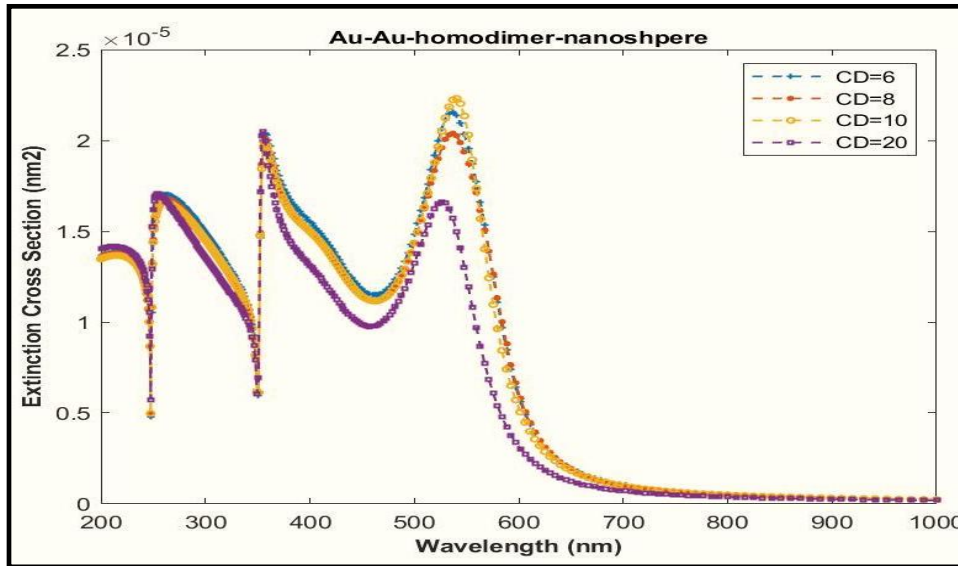


Fig. 1. Au–Au homo-dimer spectra with $d = 25\text{nm}$.

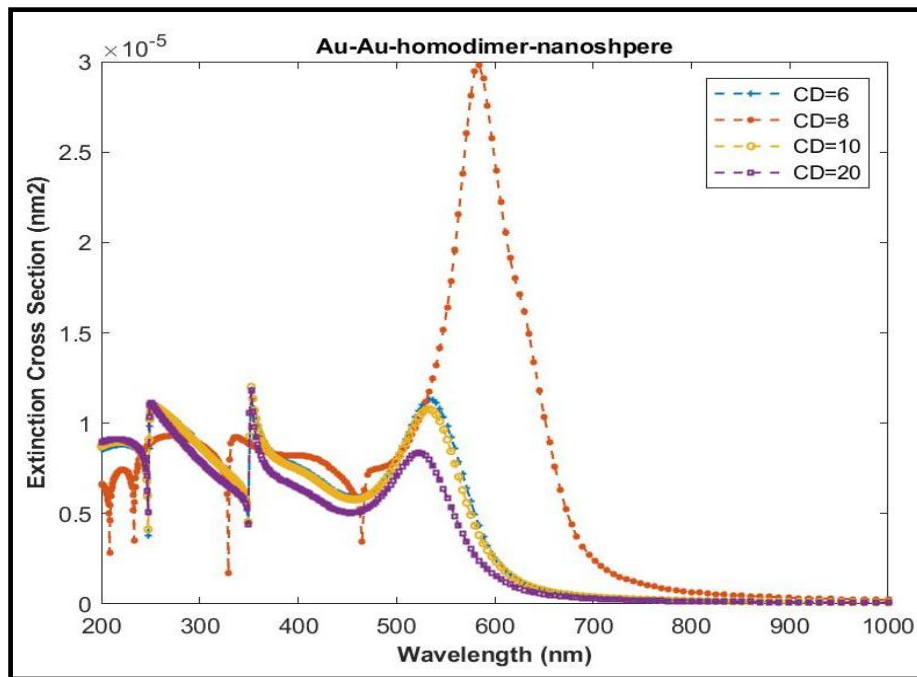


Fig. 2. Au–Au homodimer spectra with grain size = 30nm .

Au a yellowish hue, Au was the metal of choice for LSPR applications. Nickel, copper, and aluminums, with the exception of the initial metal transition, have infrequently been found to form LSPR [4].

PRINCIPLE AND SIMULATION TECHNIQUE

For the presented work, FDTD software from Lumerical FDTD solutions had been used in order to do necessary computations. With the aid of grid

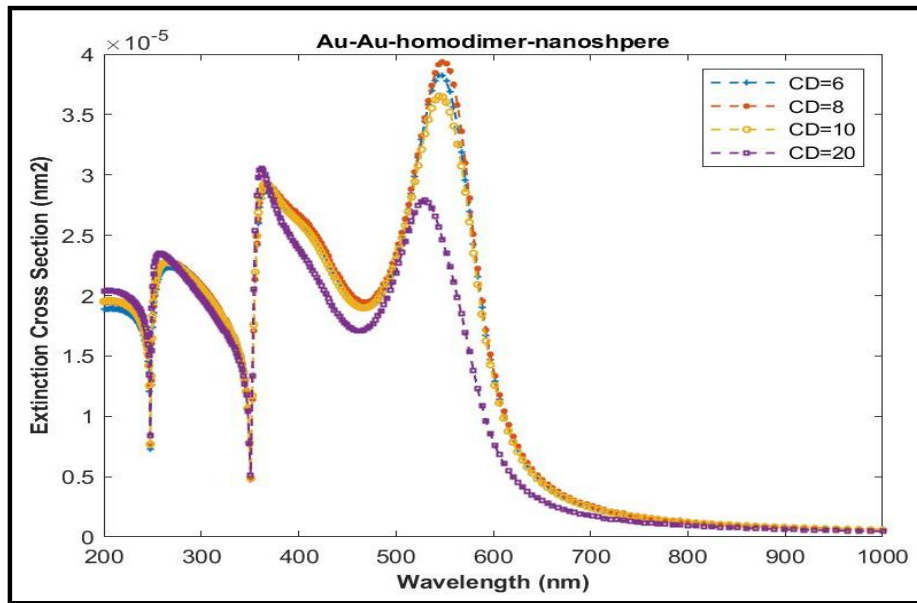


Fig. 3. Au–Au homo-dimer spectra with grain size = 35 nm.

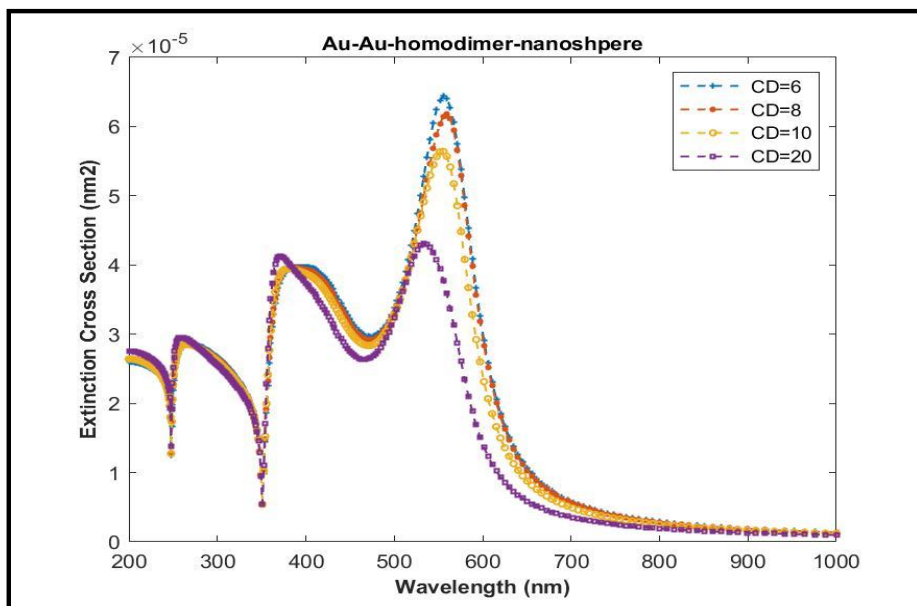


Fig. 4. Gold-gold homodimer spectra grain size = 40nm.

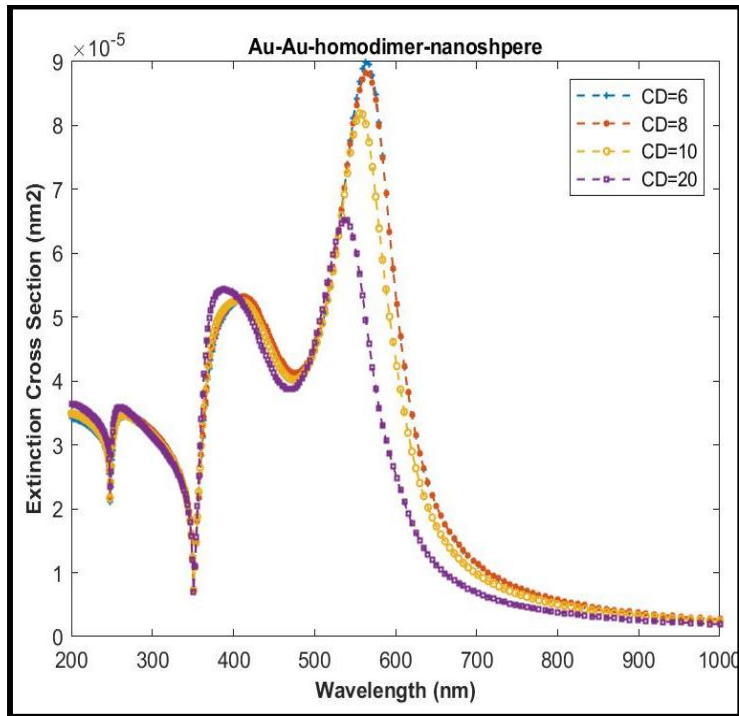


Fig. 5. Au–Au homodimer spectra with $d = 45\text{nm}$.

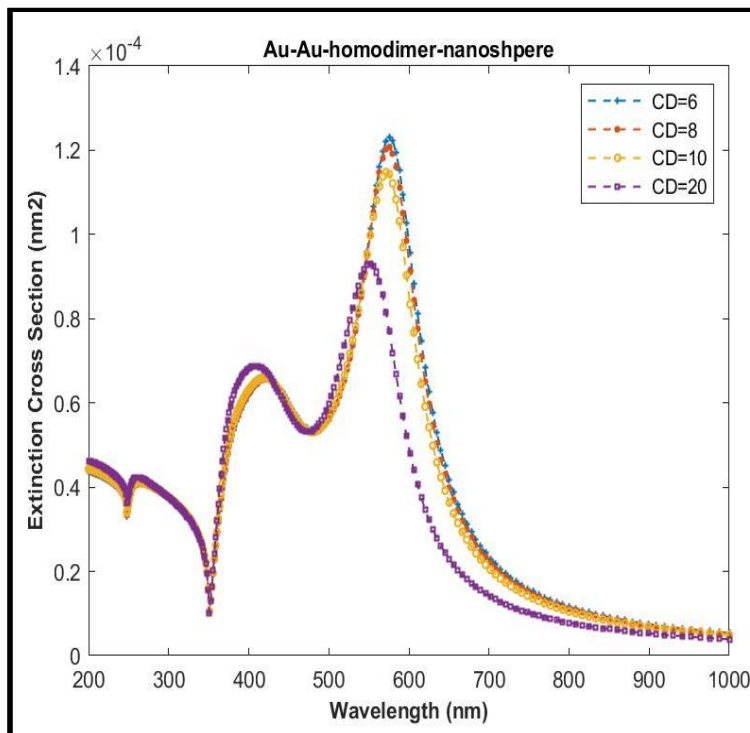


Fig. 6. Au–Au homo-dimer spectral with grain size = 50nm.

size, E-field strength must be made independent of grid size in order to carry out FDTD calculations involving Nano-spheres. Through starting with size grid of 5nm on Nano-sphere and progressively for reduced the space of grid, the method has been used until it was discovered that a further drop in the “Step size” did not have any appreciable impact on estimated values surrounding Nano-sphere. There are numerous options for lattice size in FDTD code as long as it is near the margins of the nanostructure, in which the two NPs’ CDs are 8, 6, 12, and 10 nm apart, with the first having a size of 1, 2, and 4nm.

RESULTS AND DISCUSSION

Extinction appearances of dimer

Au-Au homo-dimers

Distance between the NPs determines their interaction, as demonstrated by the measurement of two components that arise from the computation of dipole extinction spectra. (Figs. 1–6). The permittivity, size, and distance of NP (D) of permanent radius are quantitatively related to the nature of spectral distance between components. A, B, and C exhibit homo-dimer.

The spectra of extinction of gold homo-dimer with (25nm, 30nm, 35nm, 40nm, 48nm, 50nm) radius have been shown in Fig. 2 (a, b) and (c, d). Au nanosphere with distinct extinguishing spectra and d values are (6, 8, 10, and 20) nm. The extinction peak of the sample under y-polarization incident light is 598 nm. The findings have shown that the resonance wavelength almost stays constant as the interparticle separation increases. Remarkably, resonance wave-length decreases with increasing interparticle distance (d = 8 nm); yet, the resonance wavelength experiences a considerable redshift upon exposure to incident light with z polarization.[5]

In the case when the system is exposed to incident light with y-polarization, it is seen that resonance wave-length almost stays constant as interparticle space rises, with extinction peak being approximately 598 nm. When exposed to input light with z polarization, resonance wavelength is clearly redshifted and the interparticle spacing decreases to d(8nm) [6].

Ag-Ag homo-dimer

The cross section regarding Ag homo-dimer

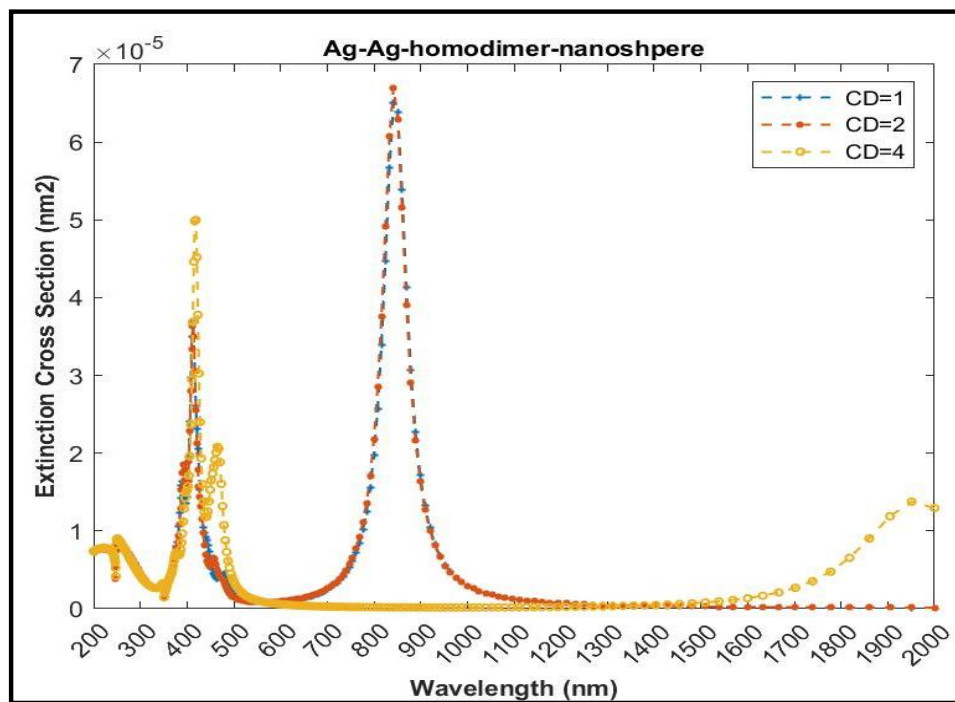


Fig. 7. Ag–Ag homo-dimer spectra with d = 30nm.

with a radius of 25nm is displayed in Fig. 7. As interparticle space covered by the simulation, as shown in Fig. 8, the position regarding the first and highest peak following illumination with y-polarization incident light is about 395nm, and resonance wavelength position is observed to be independent. However, the resonance wavelength shifts to a longer wavelength when

exposed to Z-polarization light because of an increase in interparticle spacing, Fig. 9. The Ag-Ag homodimer's extinction spectrum varies with radius, as shown in Figs. 10 and 11. Consequently, it is discovered that extinction peak's red-shift is greater under z-axis polarization compared to the under y-polarization. Thus, z-polarization occurrence is difficult, much as Ag homo-dimer

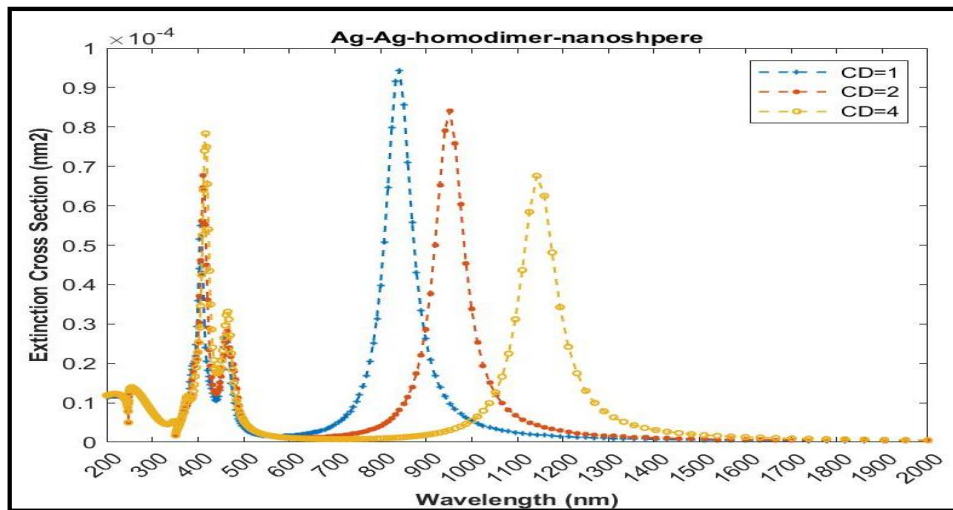


Fig. 8. Ag-Ag homo-dimer spectra with grain size = 35nm.

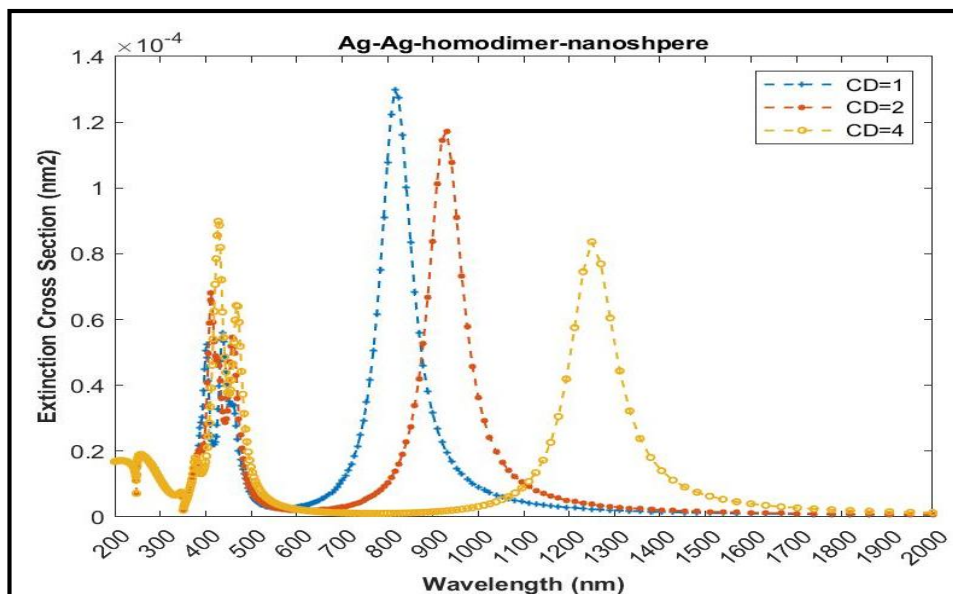


Fig. 9. Ag-Ag homodimer with $d = 40\text{nm}$.

extinction [7].

Al-Al homodimer

The geometry of the contact area for dimers consisting of 2 NPs at strong coupling plasmonic regime or low separation between the particles

has been disclosed using complementing surface-enhanced raman spectroscopy as well as scanning electron microscopy (SEM). Within this particular domain, the interparticle distance has a significant impact on optical spectra of excitation light that is polarized along dimer's main axis. Primary

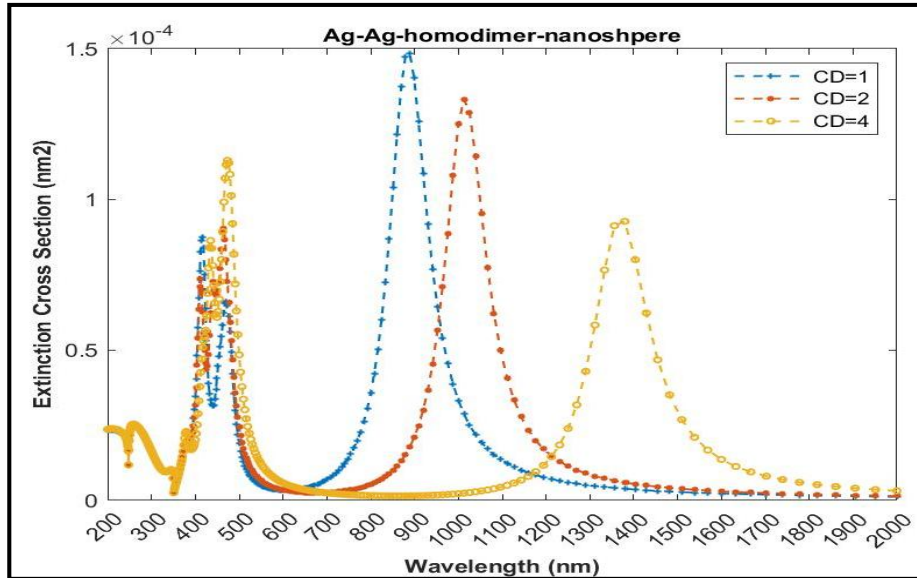


Fig. 10. Ag-Ag homo-dimer with d = 45 nm.

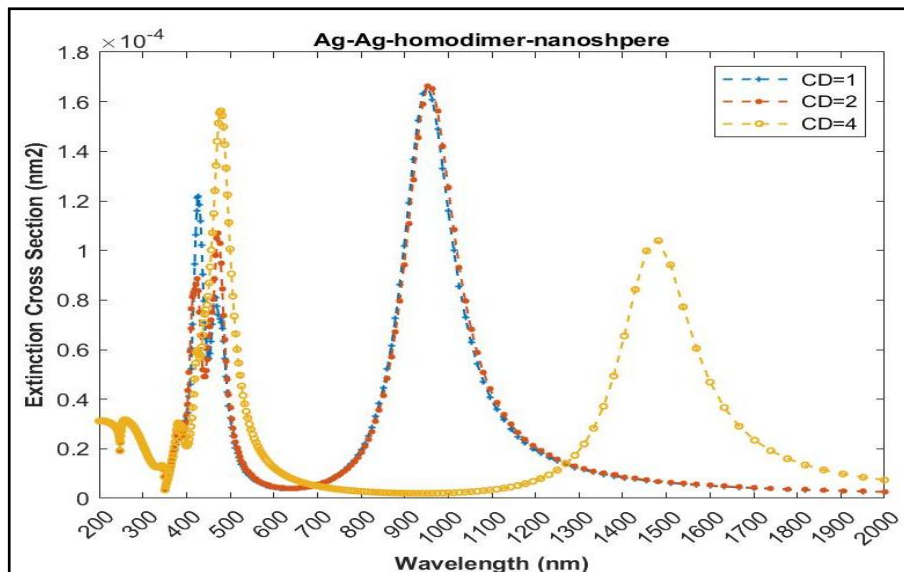


Fig. 11. Ag-Ag homodimer with d = 50.

impacts of the particle center's distance can be grouped into multiple points: the amplitude of

LSPR drops and the spectrum is "red-shifted" as the interparticle distance reduces. The based Mie

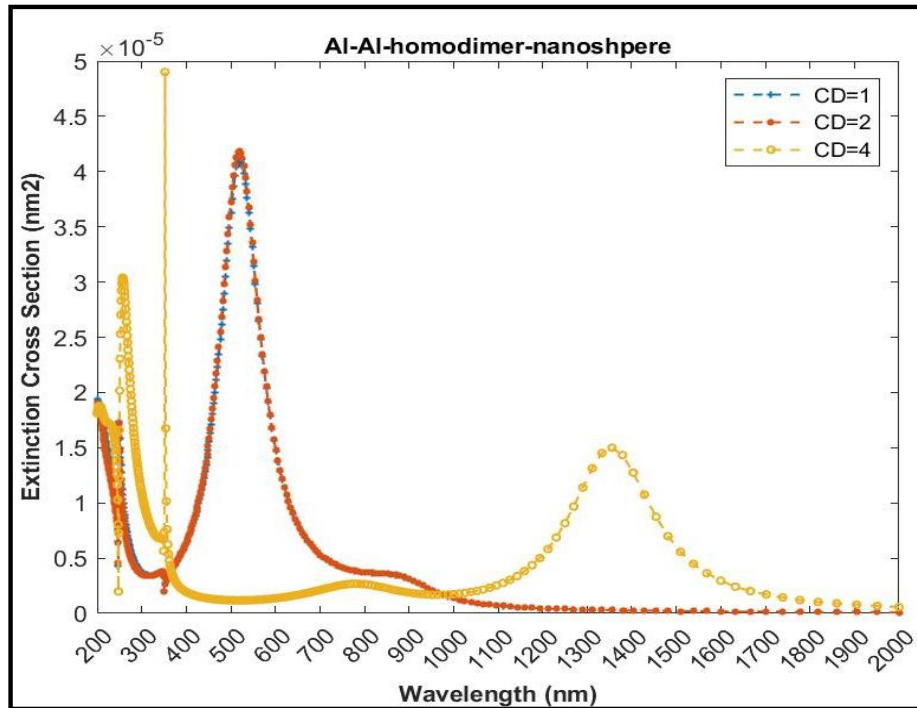


Fig. 12. Al-Al homodimer spectra with $d = 25 \sim 50$ nm.

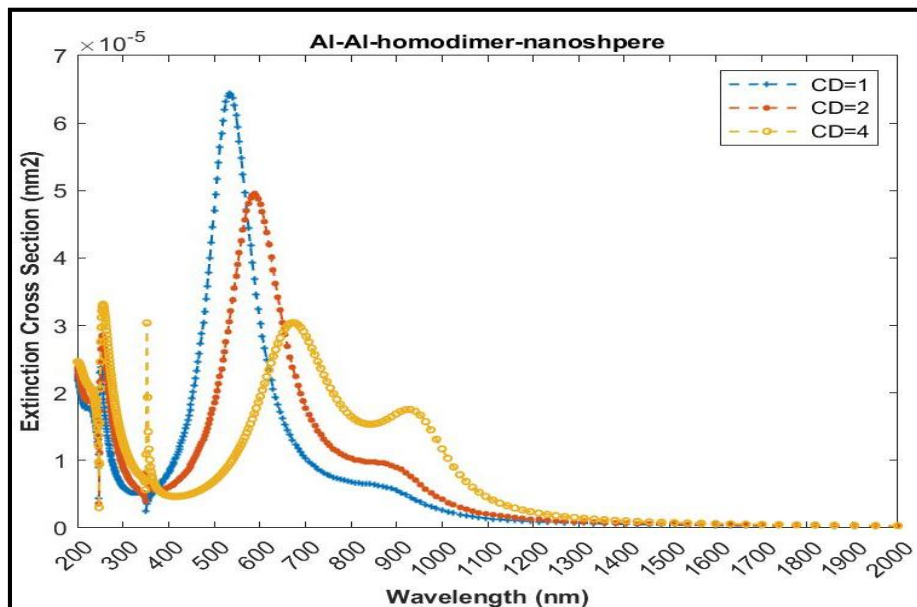


Fig. 13. Al-Al homodimer spectra with $d = 25 \sim 50$ nm.

theory result with greater extended order and the experimental results for Al dimers are found to be in very good agreement. There were, on the other hand, a few instances in which the two spectra differed, such as when there was a partial overlap (or “spill-out”) between the electron clouds of two particles. [8–9] For small interparticle distances, a replication regarding LRPS is observed in conjunction with a spectrum “hole burning” for Al nanosphere dimers. The resonance frequency of both connected NPs is strongly affected by the coupling gap and the arrangement between the two nanospheres. Typically, both coupled NPs are red-shifted with respect to localized particle Plasmon of individual nanoparticles. Al, resulting in greater localized electric fields between adjacent particles. Al NPs have a particle distance of 5 nm and diameters between 25 and 50 nm. The so-called hot spot effect, or the degree of enhancement brought about by the near field coupling between nano-particles, is plainly visible. The spectra of the linked and solitary NPs are contrasted in Figs. 12–17. These spectrum shifts for AlNPs seem to follow a general scaling equation, which is not reliant on the shape of

the particles, but on their size. The new Plasmon ruler formula for Al nanosphere pair was derived lately, highlighting the need to include multipole contributions for short distances for a broad range of interparticle distance and particle size.[10–12].

Because of the phase retardation effect, plasmon modes in the structure of a system containing NPs of different sizes and high-order (octupole, quadrupole, etc.) could readily couple with the light’s electric field; yet, we must not anticipate that electric field inside particles is homogeneous. The Surface Plasmon suffers inequality as a result of electro-magnetic interaction between localized modes, giving rise to multipole Plasmon resonances. [13]. It is suggested that in order to increase non-linear optical efficiency, such phenomena could be used in concert with an effective medium that contains the necessary particle size distribution and particle location. [14]. Fig. 18 shows the peak wavelength as well as the average particle size of the Au, Ag, and Al homodimer nanostructures, which are 25 and 50 nm, respectively. As could be observed, the nanodimer arrangement precisely illustrates the general pattern which the enhancement factor or plasmon

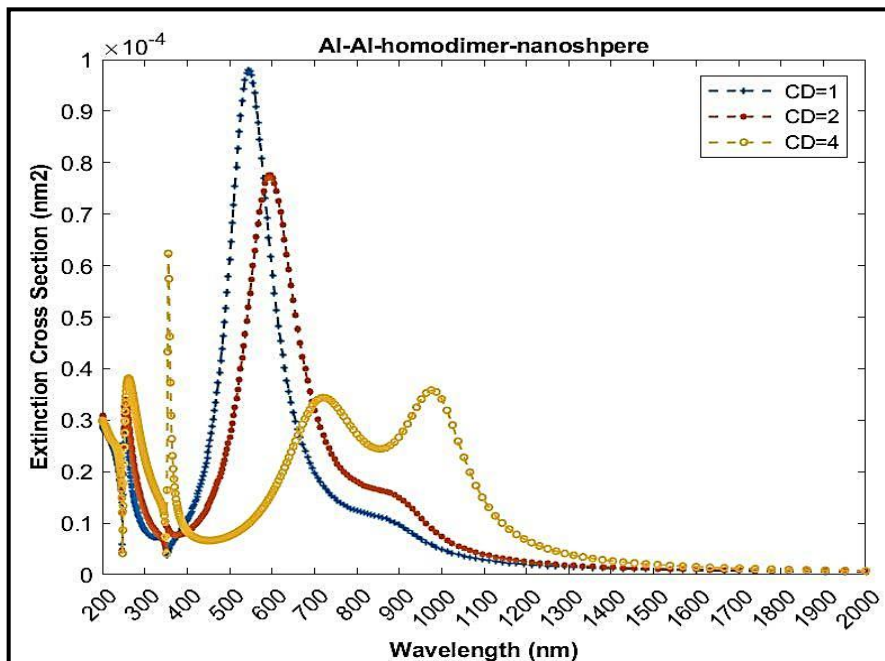


Fig. 14. Al–Al homodimer spectra with $d = 25 \sim 50$ nm.

resonance wavelength increases as it approaches the red region and grows nearly exponentially as the inter-particle distance reduces. The system's

NP exhibits a shift in surface plasmon oscillation frequency when it is coupled, relative to when it is isolated. The plasmons' near-field connection

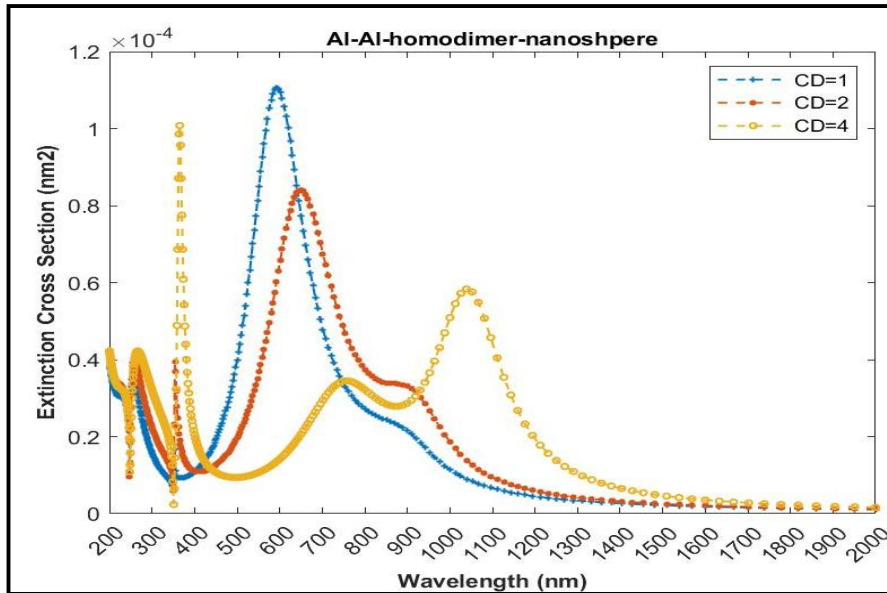


Fig. 15. Al-Al homodimer spectra with $d = 25 \sim 50$ nm.

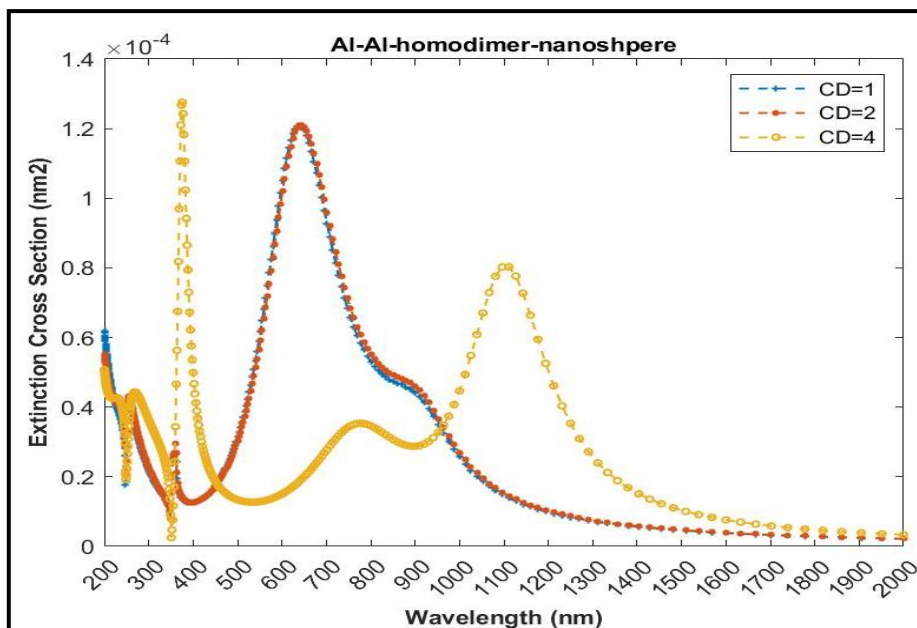


Fig. 16. Al-Al homodimer spectra with $d = 25 \sim 50$ nm.

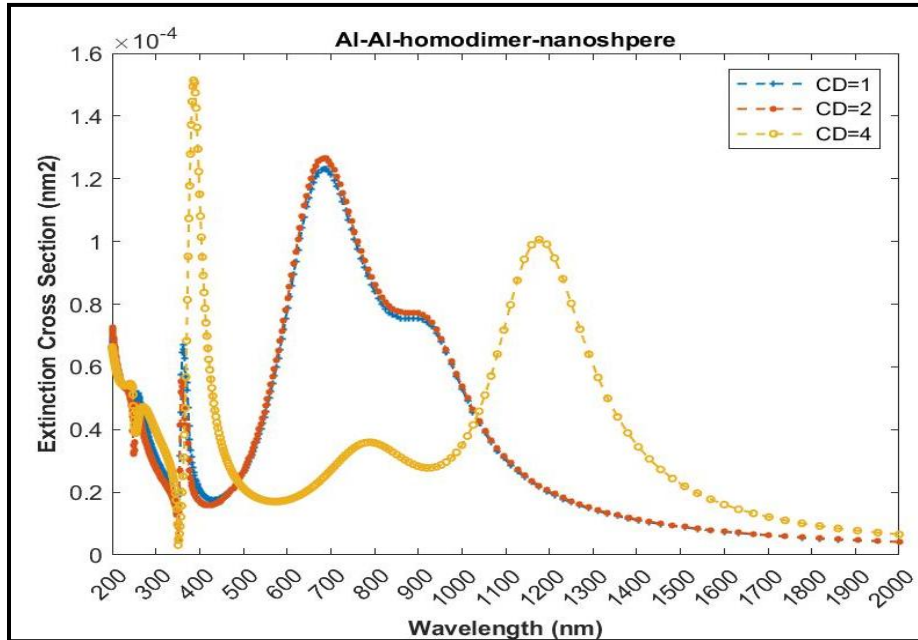


Fig. 17. Al-Al homodimer spectra with $d = 25 \sim 50$ nm.

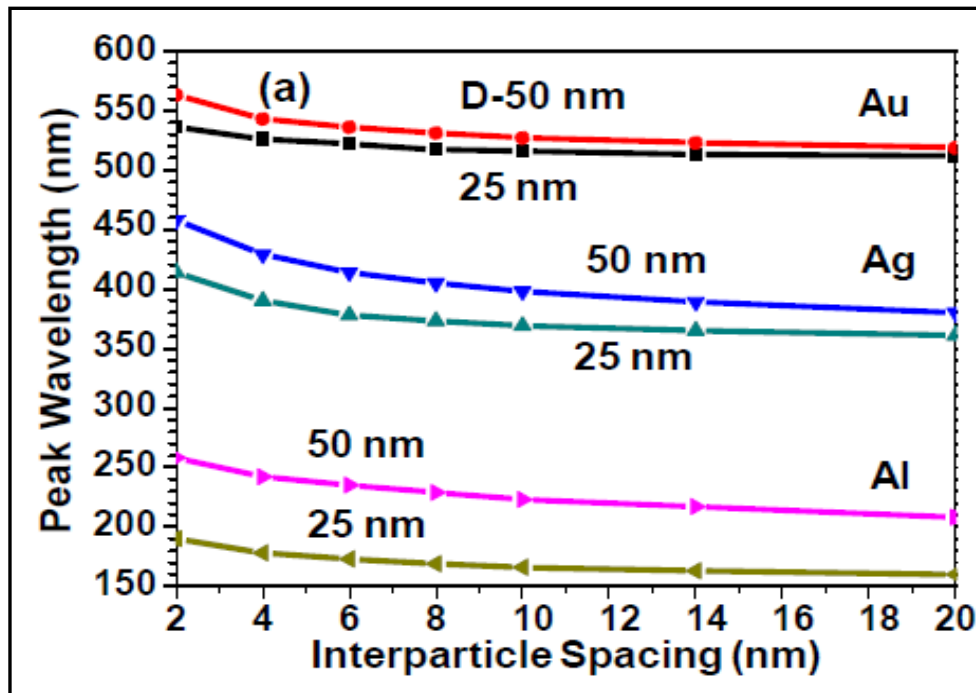


Fig. 18. Peak wave-length for homodimer nano-structures of Au, Ag, and Al (25nm) and 50nm grain size.

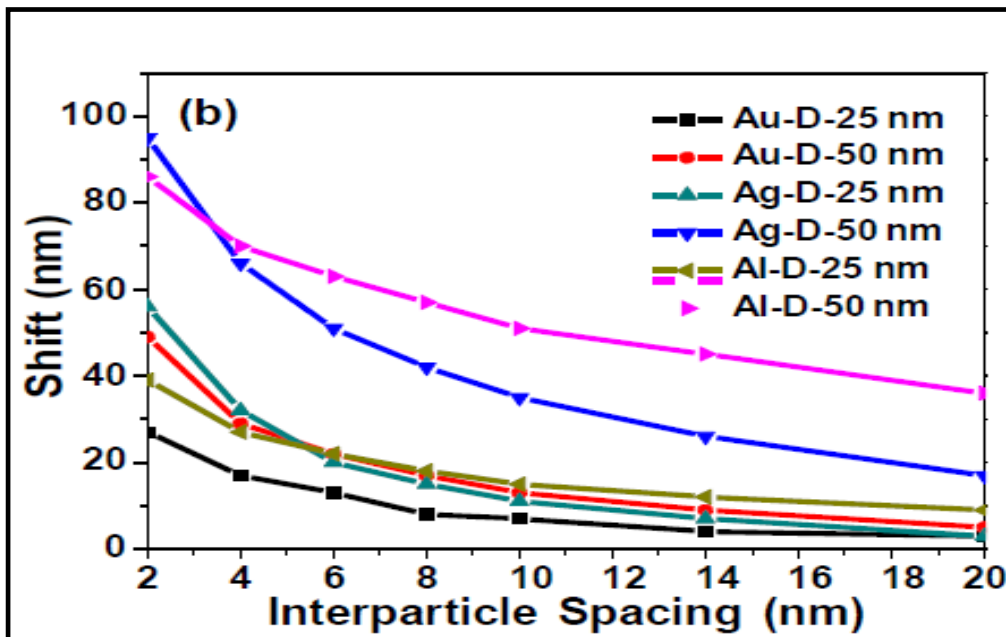


Fig. 19. Comparison of the dipole resonance wave-length of homo and homo dimer of Au, Ag and Al under varying interparticle distance. LSPR of the homo-dimer nanosphere has been experimentally and theoretically shown to vary with the interparticle spacing.

causes such particles to approach one another and interact. [15]. As the distance between particles decreases, the force for parallel polarization increases exponentially. This is because the field dimensions of particles are gradually enhanced. Simultaneous plasmon hybridization redshifts the force maximum's spectral location. [16].

The graphs illustrating the difference in a and S between the isolated nanosphere and dimer nanostructure help in illustrating how the peak wavelength changes depending on distance between the particles (the predicted shift of the peak wavelength in dependence with interparticle distance can be seen in Fig. 19). It is therefore demonstrable that Al in Pd exhibits a stronger connection than Au and Ag, leading to larger shift. Ag and Au, on the other hand, have substantially lower values, and the difference increases even more when 2 identical Al nano-spheres (D-50nm) form a dimer and cause the plasmon wavelength to shift by 36 nm. This is the case because dipoles in Al encounter a larger field than those in Ag and Au nanodimers, as shown in the layout. Because of its enhanced UV visible plasmon coupling, Al could take the role of Ag and Au NPs in a variety of applications. [17, 18].

In Fig. 19, the result can be seen from the bar

chart indicating the projected resonance wave-length of dimer for plasmon rule equation. By calculating above plot we find the value of 0.180.03 as the decay constant of an Al dimer exponential decay. Inset, we compare the behavior in the shift of the nanosphere pair that brings about plasmon coupling with the decay constant, whose value scaled by the interparticle separation divided by particle size, is nearly on the universal scaling [19].

CONCLUSION

Homo-dimer Au, Ag and Al nanosphere LSPR properties and near field in DUV-NIR area are studied through FDTD method. Both the particle size and the interparticle distance as well as the material used for the plasmonic nanostructures determine plasmon coupling which leads to the red shift of plasmon wave-length. $Al > Ag > Au$ is the coupling order from the comparison of coupling strengths of the particles which has similar geometries with Au, Ag and Al Another important thing to note is that the near field enhancement is extremely confined in the homo-dimer nano-structure. For all of materials, the intensity enhancements are ideally estimated at the contact of 108–109 at DUV–UV–visible range.

CONFLICT OF INTEREST

The authors declare that there is no conflict of interests regarding the publication of this manuscript.

REFERENCES

1. Kelly KL, Coronado E, Zhao LL, Schatz GC. The Optical Properties of Metal Nanoparticles: The Influence of Size, Shape, and Dielectric Environment. *The Journal of Physical Chemistry B*. 2002;107(3):668-677.
2. Bohren CF, Huffman DR. *Absorption and Scattering of Light by Small Particles*: Wiley; 1998 1998/04/23.
3. Jain PK, Huang W, El-Sayed MA. On the Universal Scaling Behavior of the Distance Decay of Plasmon Coupling in Metal Nanoparticle Pairs: A Plasmon Ruler Equation. *Nano Lett*. 2007;7(7):2080-2088.
4. Nordlander P, Oubre C, Prodan E, Li K, Stockman MI. Plasmon Hybridization in Nanoparticle Dimers. *Nano Lett*. 2004;4(5):899-903.
5. Prodan E, Radloff C, Halas NJ, Nordlander P. A Hybridization Model for the Plasmon Response of Complex Nanostructures. *Science*. 2003;302(5644):419-422.
6. Gao Y, Zhang R, Cheng J-C, Liaw J-W, Ma C. Optical properties of plasmonic dimer, trimer, tetramer and pentamer assemblies of gold nanoboxes. *J Quant Spectrosc Radiat Transfer*. 2013;125:23-32.
7. Wei QH, Su KH, Durant S, Zhang X. Plasmon Resonance of Finite One-Dimensional Au Nanoparticle Chains. *Nano Lett*. 2004;4(6):1067-1071.
8. Paudel HP, Bayat K, Baroughi MF, May S, Galipeau DW. Geometry dependence of field enhancement in 2D metallic photonic crystals. *Opt Express*. 2009;17(24):22179.
9. Burrows CP, Barnes WL. Large spectral extinction due to overlap of dipolar and quadrupolar plasmonic modes of metallic nanoparticles in arrays. *Opt Express*. 2010;18(3):3187.
10. Li K, Stockman MI, Bergman DJ. Self-Similar Chain of Metal Nanospheres as an Efficient Nanolens. *Phys Rev Lett*. 2003;91(22).
11. Pellegrini G, Mattei G, Bello V, Mazzoldi P. Interacting metal nanoparticles: Optical properties from nanoparticle dimers to core-satellite systems. *Materials Science and Engineering: C*. 2007;27(5-8):1347-1350.
12. Uma Rao K, Reddy CA, Chaitanya Lakshmi G, Vaishnavi G. Efficiency Enhancement of the Solar Cells through Subwavelength Scaled Biomimicked Moth Eye Patterning using Lumerical Solutions. *Materials Today: Proceedings*. 2017;4(9):10407-10411.
13. Taflove A, Hagness SC, Picket-May M. *Computational Electromagnetics: The Finite-Difference Time-Domain Method*. The Electrical Engineering Handbook: Elsevier; 2005. p. 629-670.
14. Mattiucci N, D'Aguzzo G, Everitt HO, Foreman JV, Callahan JM, Buncick MC, et al. Ultraviolet surface-enhanced Raman scattering at the plasmonic band edge of a metallic grating. *Opt Express*. 2012;20(2):1868.
15. Norek M, Włodarski M, Matysik P. UV plasmonic-based sensing properties of aluminum nanoconcave arrays. *Current Applied Physics*. 2014;14(11):1514-1520.
16. Sur UK. Surface-enhanced Raman scattering (SERS) spectroscopy: a versatile spectroscopic and analytical technique used in nanoscience and nanotechnology. *Advances in nano research*. 2013;1(2):111-124.
17. Bantz KC, Meyer AF, Wittenberg NJ, Im H, Kurtuluş O, Lee SH, et al. Recent progress in SERS biosensing. *Physical chemistry chemical physics : PCCP*. 2011;13(24):11551-11567.
18. Käll M, Xu H, Johansson P. Field enhancement and molecular response in surface-enhanced Raman scattering and fluorescence spectroscopy. *J Raman Spectrosc*. 2005;36(6-7):510-514.
19. Chowdhury MH, Ray K, Johnson ML, Gray SK, Pond J, Lakowicz JR. On the Feasibility of Using the Intrinsic Fluorescence of Nucleotides for DNA Sequencing. *The journal of physical chemistry C, Nanomaterials and interfaces*. 2010;114(16):7448-7461.
20. Chowdhury MH, Ray K, Gray SK, Pond J, Lakowicz JR. The use of aluminum nanostructures as platforms for metal enhanced fluorescence of the intrinsic emission of biomolecules in the ultra-violet. *Proceedings of SPIE--the International Society for Optical Engineering*. 2010;7577:757700-757700.
21. Singh Sekhon J, S Verma S. Refractive Index Sensitivity Analysis of Ag, Au, and Cu Nanoparticles. *Plasmonics*. 2011;6(2):311-317.
22. Jain PK, El-Sayed MA. Noble Metal Nanoparticle Pairs: Effect of Medium for Enhanced Nanosensing. *Nano Lett*. 2008;8(12):4347-4352.
23. Lin Y, Zou Y, Lindquist RG. A reflection-based localized surface plasmon resonance fiber-optic probe for biochemical sensing. *Biomedical optics express*. 2011;2(3):478-484.
24. Lin Y, Zou Y, Mo Y, Guo J, Lindquist RG. E-beam patterned gold nanodot arrays on optical fiber tips for localized surface plasmon resonance biochemical sensing. *Sensors (Basel, Switzerland)*. 2010;10(10):9397-9406.